13th ewtec 2019 Proceedings of the 13th European Wave and Tidal Energy Conference 1-6 Sept 2019, Naples, Italy

Advanced measurement and analysis of waves and turbulence using 5-, 7- or 8-beam ADCPs

Eloi Droniou, Matt Folley, Yves Perignon and Cuan Boake

Abstract—**Multi-beam Acoustic Doppler Current Profilers (ADCPs) are increasingly being used for both tidal and wave resource analysis. Two areas where multi-beam ADCPs are being used are in the analysis of currents, turbulence and waves. The performance of different ADCP beam configurations is compared, showing that using ADCPs with more than 6-beams it is possible to fully resolve the turbulence parameters. The minimum measurable Reynolds stresses is calculated for 7 and 8-beam ADCPs, correcting an error in a previous calculation by Vermeulen. Although ADCPs have long been used for tidal resource analysis, they are increasingly being used for wave resource analysis due to their suitability for relatively shallow water where wave energy converters may be deployed. The use of surface-tracking to estimate the directional wave spectrum is investigated. The need to use surface-tracking for the directional wave spectrum is particularly relevant where there are strong currents because the use of the beam-velocities for directional analysis can break-down in these circumstances. However, it is shown that weak along-beam reflections, associated with smooth water surfaces when there are light winds, results in difficulties with implementing surface tracking for slanted beams. Specifically, it is shown that reflections from directly above the ADCP could mask the weak reflection along the beam. By masking the slanted beam data using the vertical range to the surface (available from the vertical beam) the data quality could be significantly improved, although some spurious echoes remain. In addition, it was found that standard surface-tracking techniques can lead to bias in the estimate of the surface elevation and thus significant wave height due to the interpolation technique used. An alternative asymmetric interpolation technique is proposed, which is shown in significantly improve the estimate of the significant wave height when relatively large bin widths are used.**

1574. Wave resource characterization. "This work was supported in part by ADEME under grant.n°1505C0092 and by Innovate UK under project number 620116 as part of the OCEAN ERA-NET joint call fund 2014"

E. Droniou. is at DynamOcean SARL, 57 rue de Metz, 56000 Vannes, France (e-mail: eloi.droniou@dynamocean.com).

M. Folley and C. Boake are at Applied Renewable Research Ltd, 109 Gobbins Road, Islandmagee, Country Antrim, Northern Ireland, BT40 3TY, UK (e-mail: m.folley@arrltd.co.uk).

Y. Perignon is at Ecole Centrale de Nantes – LHEEA, SEM-REV, Rue de Kervenel – Parc de PenAvel, 44490 Le Croisic, France (e-mail: yves.perignon@ec-nantes.fr).

Keywords— *ADCP, Doppler, Measurement, Tidal, Reynolds stress, Turbulence, Waves*, **Echo Intensity, Surface Tracking.**

I. Introduction

A. Background

Acoustic Doppler Current Profilers (ADCP) measure water velocities throughout the water column along a number of beam directions (historically 1 to 4), as well as water surface elevations where the beams hit the sea surface. They have been extensively used in the Oceanography sector since the 1980s. They have also been used, with little or no adaptation, for the measurement of waves and currents applied to the resource assessment and characterisation of wave and tidal energies. In the 1990s and 2000s some methods were developed to characterise uncertainties [1], turbulences intensities [1] and wave influence on turbulence measurements [3].

B. Beam Velocities to Reynolds Stresses

The Reynolds stress tensor R is one of the main metrics used to characterise turbulence in a tidal stream flow. It is composed of 3 normal stresses and 3 shear stresses:

$$\mathrm{R} = \rho \begin{pmatrix} \overline{u'^2} & \overline{u'v'} & \overline{u'w'} \\ \overline{u'v'} & \overline{v'^2} & \overline{v'w'} \\ \overline{u'w'} & \overline{v'w'} & \overline{w'^2} \end{pmatrix} \quad (1)$$

ρ water density

u', v', w' turbulent velocity fluctuations along x, y, z axes

The turbulence techniques were however limited by the maximum of 3- or 4-beams which only allowed calculating the vertical shear stresses. The TKE was then estimated using an assumed constant value of the anisotropy ratio $\alpha = 0.2$ as in [1] which was introduced by [2] for an unstratified tidal channel. This assumption was however shown to be inappropriate in [6], [7]. The use of 5-beam arrangement either ad-hoc [4], [5] or off-the-shelf allowed to calculate the TKE and the anisotropy ratio. However, the horizontal shear stress $\overline{u'v'}$ remained unknown. It was therefore required to use 6-beams or more to calculate the full Reynolds stress tensor. Ad-hoc or off-the-shelf configurations of 7- and 8-beam are possible and will be discussed in section III.

C. *Wave measurements*

Waves can be analysed from ADCP data using three different sources:

- One pressure measurements at the instrument head
- Four or five beam velocities at a selection of 3 to 5 bins just below the layer contaminated by the side-lobes
- Four or five surface elevations where the beams hit the surface, obtained from the peak of the echo intensity

A vertical beam improves significantly the analysis of the 1D frequency spectrum providing direct measurement of vertical component of the orbital velocities and reducing noise and bias for the estimation of the surface elevation.

The surface elevation measurements may be unreliable for two extreme cases. During events of swell and light winds, Terray et al [9] identified that under such smooth surface conditions, the scattering is mostly specular, making it difficult to differentiate the main and side-lobe returns. During events of breaking waves, air bubbles below the surface may also bias low the detection of the sea surface. For these reasons the analysis of wave spectra from beam velocities has been favoured, at least for the slant beams. The vertical beam is indeed not much affected by the light wind conditions. This is the strategy used in proprietary software from ADCP manufacturers when a vertical beam is available.

However Droniou et al [7] found that in the presence of a strong ambient current, the analysis method using beam velocities, in Teledyne RDI's WavesMon software, fails due to the difficulty of handling the effect of current within the transfer function between the beam velocity and the surface elevation. Also turbulence, common within a strong tidal stream site, combined with the Doppler noise, leads to a low signal to noise ratio for the wave spectrum obtained from the beam velocities. For tidal stream energy sites, we therefore recommend to use surface elevation measurements from the ADCPs.

Detection of the peak of the echo-intensity and its interpolation are included in WavesMon. Historically this was used only to calculate the non-directional spectrum. Recently some directional analysis has also been introduced.

D. *Aims*

The aims of this paper are to discuss the collection of new 5- and 8-beam ADCP data with a vertical beam (section II), discuss the various beam configurations and their implications on measurement of waves and Reynolds stresses (section III), and improve the detection and interpolation of the peak of the echo intensity corresponding to the free surface (section IV) to obtain improved waves results (section V).

II. DEPLOYMENTS

E. *Study Site*

SEM-REV sea test site is an experimental facility operated by Ecole Centrale Nantes for the full scale testing of marine structures and equipment related to marine renewable energy. The test site is located 10 nautical miles offshore Le Croisic, France. This site has a wide range of wind and waves conditions. It also has small currents with spring peak velocity of 0.5 m/s. The water depth is homogeneous across the site at 33 m chart datum. Mean spring tidal range is circa 5 m. It has a permanently moored Datawell directional wave rider buoy MkIII and a wind sensor on the nearby "Grands Cardinaux" lighthouse. It is therefore ideal to develop the new waves measurements methods with a small ambient current and validate against the buoy data.

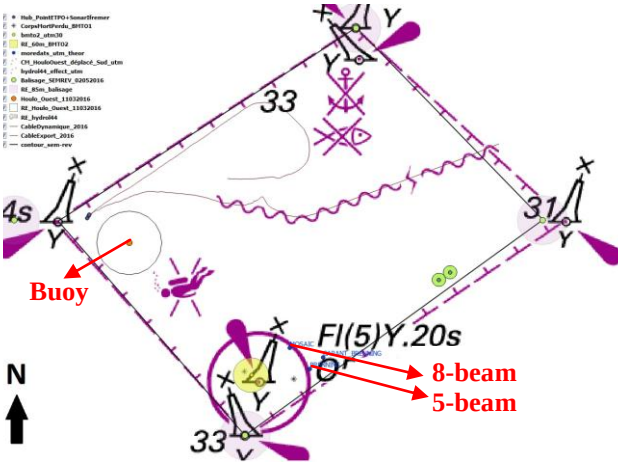

Fig. 1. SEM-REV site area delimited by the four special mark buoys. The two ADCPs are 100 m apart and 700 m away from the wave buoy.

F. *Acoustic Doppler Current Profilers*

Waves measurements were obtained using two ADCP configurations, each within its own seabed platform: one 5-beam and one 8-beam configuration. The two ADCPs were 100 m apart and 700 m away from the wave buoy (Fig. 1)

The 5-beam unit was an off-the-shelf Teledyne RDI Sentinel V50 as shown in Fig. 2 (a). It was set to perform 2 different pings within 1.00 s ping 1 and ping 2 with 100 cm and 50 cm depths cells respectively. Each ping was composed of a sub-ping of the four slant beams followed by a sub-ping of the vertical beam.

The two pings with different bin size were chosen to support a sensitivity study of the bin size on the quality of surface elevation analysis. If averaging ping 2, two bins by two bins, it is almost equivalent to ping 1 and the data acquisition time step can be considered as 0.50 s.

The 8-beam unit was made of two Teledyne RDI Workhorse 600 kHz in the same orientations as in [6] as shown in Fig. 2 (b). The two ADCPs are synchronised with the "master-slave" configuration. Due to the relatively large depth, if setting the ADCPs to ping at

0.50s it would keep lagging. Indeed time between pings was 0.52 s most of the time but varying between 0.51 s and 0.57 s. Occurrences of isolated longer time between pings (0.57 s) are supposed to correspond to the ADCP emptying its memory buffer. Using some optimisation of the command ping rate and the offset between slave and master pings (0.10 s), it was possible to improve the regularity of the ping rate: 0.51 s most of the time with some occurrences of 0.50 s and 0.52 s.

(a) BRENNIG seabed platform with one Sentinel V

(b) MOSAIC seabed platform with two coupled ADCPs

Fig. 2. ADCPs used for measurements.

TABLE I
ADCP CONFIGURATIONS

	5-beam	8-beam
Platform Name	BRENNIG	MOSAIC
ADCP	Teledyne RDI Sentinel V	Teledyne RDI Workhorse (x2)
Acoustic frequency	500 kHz	600 kHz
Vertical cell size	100 and 50 cm	120 cm
Time between pings	0.50 s	0.51 s
Slant beam angle	25°	20° to 40°
Start Date	08/10/2016	08/10/2016
End Date	16/11/2016	09/11/2016

During the ADCP measurements (32 to 39 days), the significant wave height was mostly around 1 m with four more energetic events reaching 1.5, 2.0, 1.5 and 3.5 m (Fig. 3)

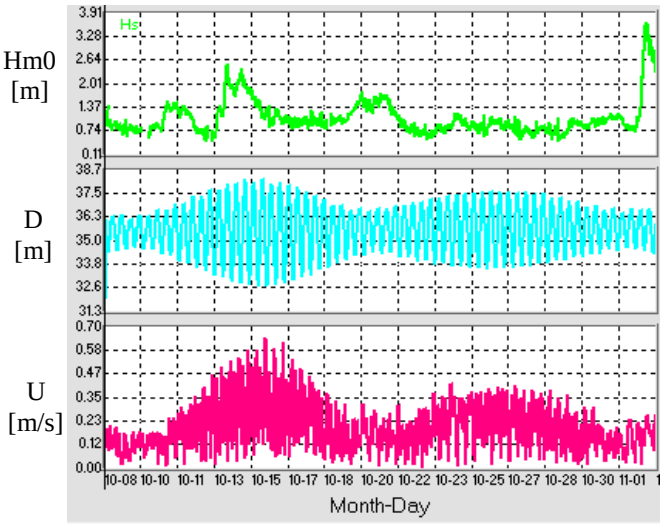

Fig. 3. Overview of wave height (Hm0 [m]), water level (D [m]) and current velocity magnitude (U [m/s]) from the 8-beam ADCP.

III. ADCP BEAM CONFIGURATIONS

In the early 2010s, some 8-beam arrangement, with two coupled 4-beam ADCPs, were used by Vermeulen et al. [6] who introduced this configuration and its associated analysis technique for tidal flows with weak current velocities < 1 m/s. The methodology was also applied to tidal energy studies with peak velocities > 3 m/s [7] and [8]. Having 6 beams or more allows calculating all 6 Reynolds stresses without any bias proportional to tilts. The coupled ADCP arrangement allows many beam configurations choosing the relative yaw and tilt angles of the 2nd ADCP relative to the 1st ADCP. The typical configuration devised by [6] corresponds to yaw = 45° and pitch = 20°. It has the advantage of having a vertical beam providing direct measurement of w and therefore $\overline{w'^2}$ when the ADCP is level. The coupled ADCP technique has some disadvantages:

- if using all 8 beams, one of the beam is slanted by 40° which reduces the valid range to 77% instead of 90% or 94% for the 20° or 25° slanted beams respectively
- the uncertainties in the mechanical mounts of the two ADCPs induce uncertainties in the equations to solve Reynolds stresses
- the two units are synchronised to interleave the pings and minimise ping-to-ping interferences. Sending and receiving the synchronising trigger adds to the signal processing overheads and it is challenging to reach constant 2Hz sampling within water depths > 30 m
- the seabed platform to host the two ADCPs must be larger than for a single ADCP and makes it difficult to have the whole 8-beam system within a single gimbal
- the setup with larger frame and two ADCPs is more expensive than for, e.g. a 5-beam setup

TABLE II
COMPARISON OF THE DIFFERENT BEAM CONFIGURATIONS

Examples	Configuration	Ping sequence	TKE $\overline{w'^2}$	$\overline{u'^2}$ $\overline{v'^2}$	$\overline{u'w'}$ $\overline{v'w'}$	$\overline{u'v'}$	% of Water Column	Vertical Beam	Cost
		3 + 1	Vertical instrument only	✗	Errors proportional to tilts and unresolved terms	✗	>90	✓	+
		4	✗	✗		✗	>90	✗	+
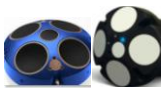		4 + 1	✓	Instrument coordinates only		✗	>90	✓	+
		3 + 3 + 1	✓	✓	✓	✓	>90	✓	++
		4 + 4	✓	✓	✓	✓	>90	✗	++
	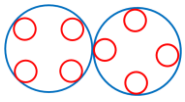	4 + 4	✓	✓	✓	✓	77	✓	+++

Some 7- and 8-beam ADCPs are now available off-the-shelf[1], providing a solution to get all 6 stresses with an easier and cheaper setup. The characteristics of the different beam configurations are summarised in Table II.

The minimum measurable stresses, as calculated with the method by [6], but revised and extended in Appendix A, are given for different 7- or 8-beam configurations (Table III). The 8-beam configuration with regular azimuth and constant slant angle gives the smallest uncertainties overall. However, the differences are small across the various configurations and the advantage of the vertical beam probably makes the 7-beam configuration the best compromise.

TABLE III
MINIMUM STRESS THAT CAN BE DETECTED USING AN AVERAGING INTERVAL OF 20 MINUTES

Configuration	Minimum measurable stress (Pa)					
	$\rho\overline{u'^2}$	$\rho\overline{v'^2}$	$\rho\overline{w'^2}$	$\rho\overline{u'v'}$	$\rho\overline{u'w'}$	$\rho\overline{v'w'}$
	0.19	0.19	0.02	0.19	0.03	0.03
	0.43	0.43	0.04	0.22	0.04	0.04
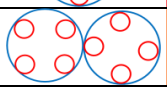	0.28	0.28	0.04	0.19	0.04	0.04

[1] Rowe Tech Inc: SeaSEVEN (7-beam) and Dual Frequency (8-beam)

IV. WAVE METHODS

G. *Estimating directional wave spectra using an ADCP*

Traditionally, the measured along beam water particle velocities have been used to estimate the surface waves at the location of the ADCP. Specifically, the along beam velocities have been related to local surface elevations based on the linear wave theory. Linear wave theory assumes that waves can be represented as the linear super-positioning of a finite number of sinusoidal waves with individual frequencies, amplitudes, directions and phases. In this case, the along-beam velocities can be directly related to the surface elevation, where for each frequency component the water-particle velocity is proportional to the product of wave frequency and the depth dependent amplitude of motion, which in deep water decays exponentially with depth as a function of the wave number. The transfer function required to convert the measured water particle velocities to surface elevation is simply the inverse of the surface elevation to water particle velocity transfer function. The directional wave spectra can then be calculated using the estimated surface elevations associated with the four or more ADCP beams using one of the available directional analysis techniques, such and the Iterative Maximum Likelihood Method (IMLM), which is used in a number of commercial analysis packages.

In many circumstances this approach has been found to provide a good and reliable estimate of the wave spectrum, which justifies its use and resilience. However, there are also circumstances where this technique breaks

down, one of which is where there are strong currents. The method fails because in strong currents the encounter frequency is not the same as the intrinsic frequency for the waves; waves travelling with the current will appear to have a higher frequency (for a stationary observer) than waves travelling against the current. Thus, it is not possible to determine directly the wave intrinsic frequency, which is required to calculate the water velocity to surface elevation transfer function, without knowing the direction the wave is travelling in. But the directional spectrum cannot be estimated without knowing the surface elevations. Thus, the traditional method for directional wave analysis breaks down in strong currents. However, ADCPs do not need to use the water velocity to estimate the surface elevation but can measure it directly using the beam echo intensity. This is possible because the air-water interface at the ocean surface is a good reflector and so the distance to the surface can be defined by a peak in the echo intensity. By measuring the surface elevation directly, there is no need for a frequency-dependent transfer function and so it should be possible to estimate the directional spectrum using this method even where there are strong currents (with, if necessary, a minor modification to the directional analysis to account for the change in wave phase velocity due to the marine currents). Clearly, the performance of this method depends on the ability to identify the correct peak in echo intensity and to determine its location accurately.

H. Peak Detection

In ideal circumstances the detection of a peak in a signal is simple; you find the largest value, and this represents the peak. Unfortunately, whilst this may work in many circumstances the surface-track data from the 5-beam ADCP deployment clearly shows that this will not always be true as illustrated in Fig. 4.

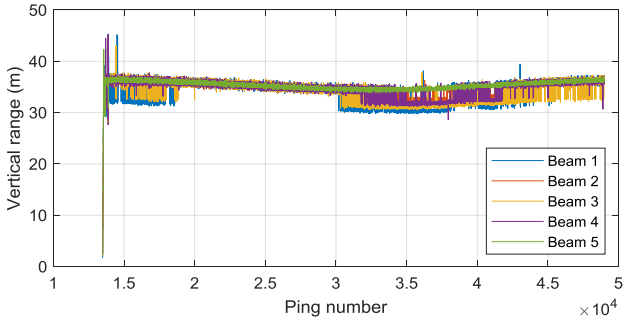

Fig. 4. Surface-track data from 5-beam ADCP deployment.

In this case, the vertical beam (Beam 5) provides a good track of the surface, whilst the slant beams appear to be working acceptably at times, but with a near constant offset at other times. Indeed, the offset of the estimated vertical distance to the surface between the Vertical and slant beams is very close to constant as illustrated in the detail from the same data shown in Fig. 5 indicating that they are coming from the same source, which is the surface directly above the ADCP.

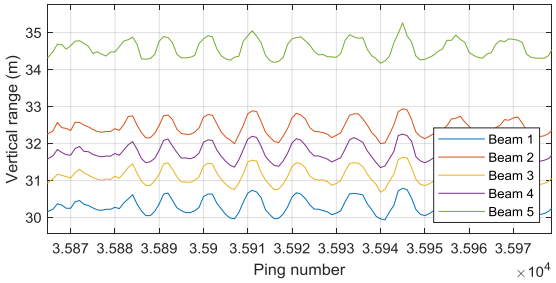

Fig. 5. Detail of surface-track data from 5-beam ADCP.

Further evidence to support the hypothesis that the data for the slant beams is actually from a point directly above the ADCP is to consider what error in the distance to the surface this would produce, which is given by (1)

$$\varepsilon = D(1 - \cos\theta) \tag{2}$$

ε error in vertical distance
D vertical distance to water surface
θ beam angle

In this sub-set of analysed data, the ADCP has almost constant roll (-1.2°) and pitch (+4.1°) angles, which needs to be added/subtracted from the 25° slant beam angle to provide the actual beam angle. Table IV shows the potential error in the vertical distance. This Table also contains an estimate of the error in vertical distance based on Fig. 5, which is very similar to the calculated error in vertical distance.

TABLE IV
ACTUAL AND ESTIMATED ERRORS IN DISTANCE TO SURFACE COMPARED

Beam number	Beam Angle	Calculated error	Estimated error
1	29.1	4.4 m	4.3 m
2	20.9	2.3 m	2.2 m
3	26.2	3.6 m	3.5 m
4	23.8	3.0 m	2.9 m

It appears that the strength of the echo recorded from the surface directly above the ADCP is stronger than the echo recorded along the beam. The tendency for this case to arise will depend on the directional sensitivity of the slant beam transducer and the intensity of the echo that goes back towards its source (the ADCP).

The design of the ADCP beams is such that they are highly directional and at 25° away from the axis of the beam, the beam intensity is typically reduced by at least 35 dB leading to a 70 dB reduction for the 2-way echo, which equates to being 10,000,000 times weaker relative to the beam axis. Fig. 6 shows the echo intensity for cases of when the surface track is working correctly - (a) and for when it incorrectly tracks the surface directly above the ADCP - (b). The spurious echo from directly above the ADCP can also just be seen in Fig. 6 (a), but in this case it is weaker than the echo in-line with the beam axis and so the correct peak is detected.

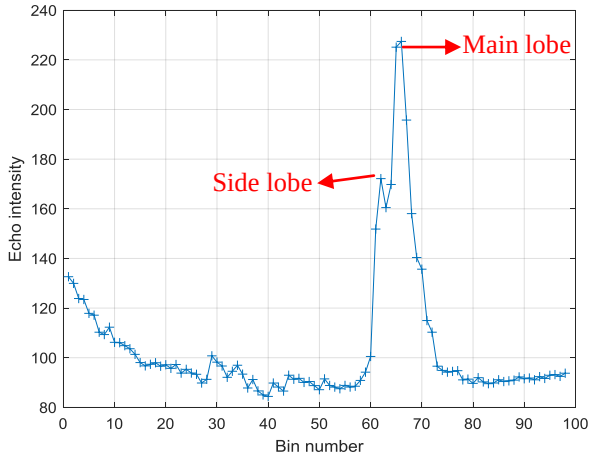

(a) Correct peak detection

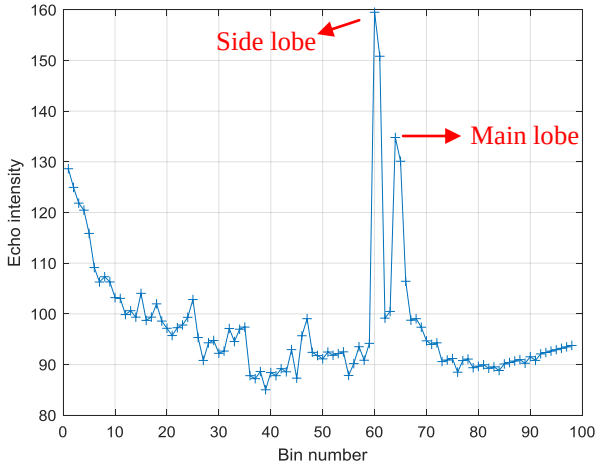

(b) Incorrect peak detection

Fig. 6. Example echo intensities for a slant beam.

A particularly low echo intensity for a slant beam can occur when the surface is glassy. As has already been noted, in this case the reflection will be almost completely specular so that the angle of reflection is equal to the angle of incidence, so that virtually no energy returns along the axis of a slant beam as illustrated in Fig. 7.

A glassy water surface typically occurs when there is a low local wind speed and so the prevalence of erroneous peak detection can be expected to be correlated to the local wind speed. This is illustrated in Fig. 8, where it can be seen that at low wind speed the percentage of good data, where the correct peak is detected, reduces significantly.

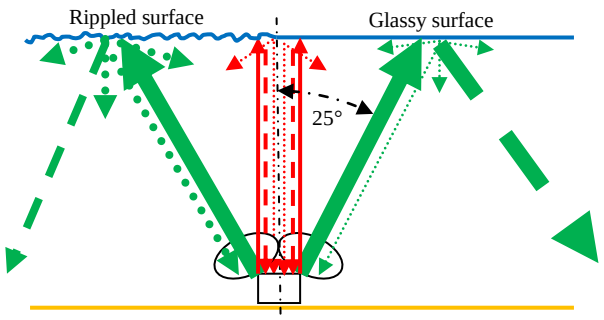

Fig. 7. The main-lobe (green) has enough echo (dotted line) when sea surface is rippled (left side). The side-lobe echo (red) may be stronger than the main-lobe echo if the reflection is mostly specular (dashed line) when the sea surface is glassy (right side).

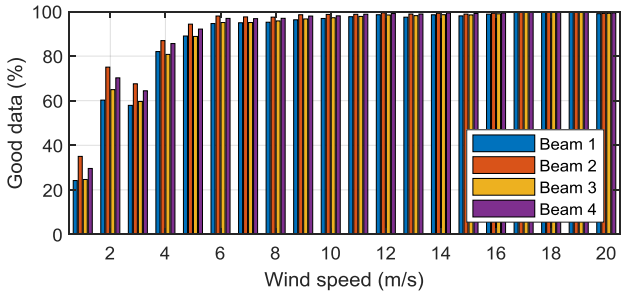

Fig. 8. Variation on return of good surface-track data with wind speed.

Although the wind speed could be used to identify periods of dubious surface-track data, an alternative approach is to mask the echo from the range associated with the vertical distance to the surface directly above the ADCP, which is available from the fifth beam. The result of this masking is shown in Fig. 9 for the same data as that given in Fig. 4. This shows a significant improvement in the performance of the surface-tracking from the slant beams, although there still remain periods where it appears that spurious echoes contaminate the surface-track data.

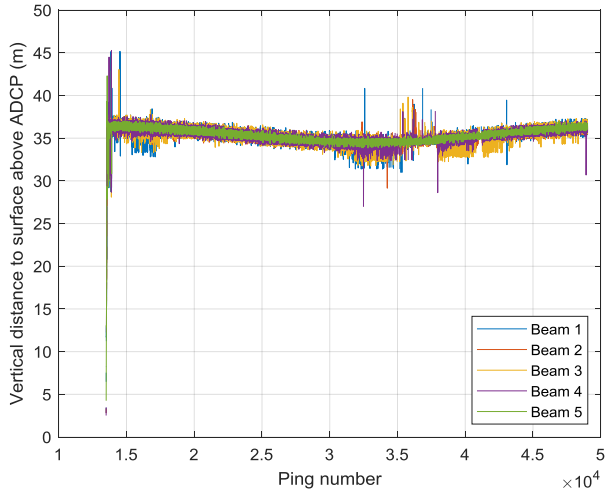

Fig. 9. Improvement in slant beam surface-track data using masking of spurious echo.

I. Peak interpolation

Once the bin with the largest echo intensity has been identified it is necessary to interpolate the echo intensity to provide a more accurate estimate of the distance to the surface. Without interpolation the resolution of the surface-track would be equal to the bin height, typically 50 – 150 cm, which would not provide sufficiently accurate surface elevation data for wave spectral analysis. Few details are typically given for the interpolation methods that are used in surface tracking algorithms, but the selection of an appropriate interpolation technique is important to achieve an accurate and unbiased estimate of the surface elevation. Two common methods of peak interpolation for ADCPs are 'linear' interpolation, which is used by the RDI WavesMon software, and 'quadratic' interpolation, which has been proposed by Terray et. al. [9]. In both methods the largest echo intensity is used with the echo intensity for the two adjacent bins to

identify a peak. Both methods are illustrated in Fig. 10, which shows that in general the two methods produce different estimates for the range to the surface.

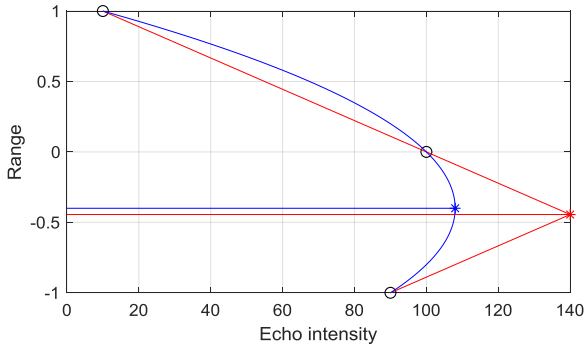

Fig. 10. Linear and quadratic interpolation.

Data from the vertical beam of the 5-beam ADCP has been used to assess the potential bias for both the 'linear' and 'quadratic' peak interpolation techniques for both the Ping 1 data, which has a bin height of 100 cm and the Ping 2 data, which has a bin height 50 cm. The probability distributions for the surface location estimated using these two interpolation techniques are illustrated in Fig. 11

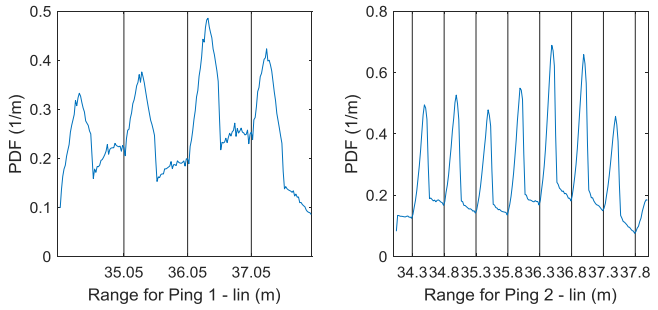

(a) Linear interpolation

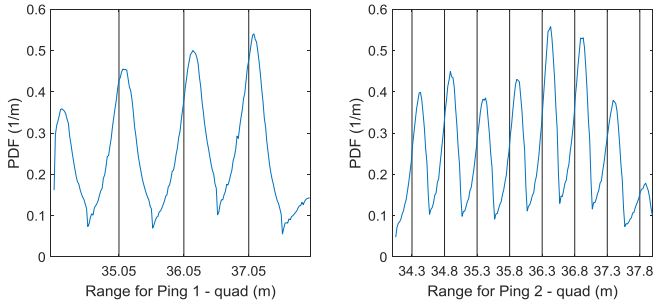

(b) Quadratic interpolation

Fig. 11. Probability distributions for interpolation techniques.

The vertical lines in Fig. 11 show the bin centres, and it is clear that both methods bias their estimates of the surface location to these bin centres. This is not too much of an issue when the variation of the surface elevation is much larger than the bin size, but can cause significant errors in the estimation of wave characteristics when the waves are small relative to the bin size. This is illustrated in Fig. 12 where the estimate of the significant wave height using the Ping 2 data (100 cm bin height) is much more variable than the estimate obtained using the Ping 1 data (50 cm bin height).

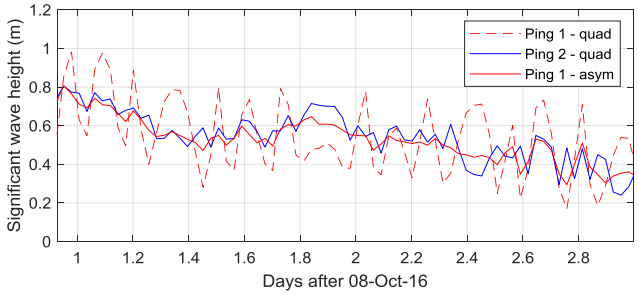

Fig. 12. The estimate of significant wave height for different bin sizes and interpolation techniques.

Fig. 12 also illustrates the use of a third interpolation technique that is based on asymmetrical linear interpolation. Asymmetrical linear interpolation is based on the recognition that the gradient of the echo intensity is not the same either side of the peak and so the interpolation technique should allow for this asymmetry. Unfortunately, the asymmetry in the echo intensity peak varies with deployment conditions and so cannot be defined directly. However, an estimate of the asymmetrical nature of the peak can be obtained by assuming that the conditions are constant during the sample used for estimating the wave conditions, typically 20 – 40 minutes. Then the steepness of the slopes either side of the peak can be estimated using a least-squares minimisation, the details of which are provided in Appendix B. It can be seen in Fig. 12 that this asymmetric linear interpolation provides an estimate of the significant wave height that is as accurate as for the quadratic interpolation for the 50 cm bins but using the 100 cm bin data.

Although the asymmetric linear interpolation provides a better estimate of the surface track for this case, it is still far from the correct model as can be seen in its own probability distribution as illustrated in Fig. 13

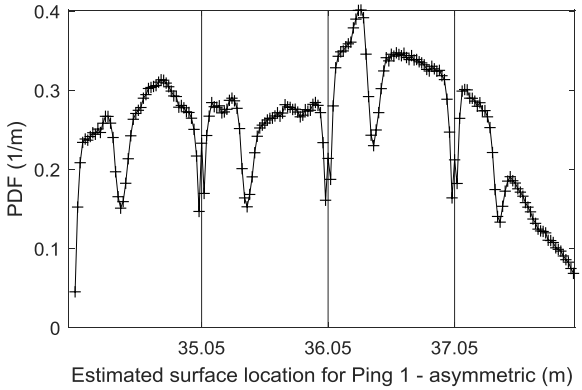

Fig. 13. Probability distribution for asymmetric linear interpolation.

V. WAVE RESULTS

The performance of the quadratic and asymmetric linear interpolation techniques is assessed by comparing the estimates of the significant wave height and energy with those from the Waverider buoy deployed locally. The statistics for the estimates are provided in Tables V

and VI. These show that for the 100 cm bins the asymmetric linear interpolation has much less uncertainty compared to the quadratic interpolation for the significant wave height Hm0, but for the 50 cm bins there is little gain in accuracy, but has little effect on the accuracy of the estimate of the energy period, Te. Moreover, the remaining differences with the buoy can largely be attributed to the uncertainty implied by the sampling variability for record length of 40 minutes and sensors located about 700 m apart. A cross comparison of measurements performed by two Mk3 buoys moored 1km apart – same West buoy compared to measurements made at east corner over the site during year 2012 – demonstrated a Scatter-Index in the order of 7% for Hm0 [11].

TABLE V
STATISTICS FOR H_{M0} RELATIVE TO BUOY DATA

	Ping 1 quadratic	Ping 2 quadratic	Ping 1 asymmetric	Ping 2 asymmetric
Mean diff.	0.024 m	0.025 m	-0.001m	0.005 m
Std. diff.	0.128 m	0.082 m	0.092 m	0.083 m
N. Std.	0.19	0.11	0.11	0.10

TABLE VI
STATISTICS FOR T_E RELATIVE TO BUOY DATA

	Ping 1 quadratic	Ping 2 quadratic	Ping 1 asymmetric	Ping 2 asymmetric
Mean diff.	0.37 s	0.20 s	0.43 s	0.28 s
Std. diff.	0.50 s	0.44 s	0.50 s	0.45 s
N. Std.	0.078	0.063	0.078	0.067

VI. CONCLUSIONS

In this paper, we have first reviewed some ADCP beam configurations considering their advantages for the characterisation of waves and turbulence. We then used 5- and 8- beam ADCP measurements, collected at an offshore test site exposed to swell, to improve the waves analysis methods using surface elevations instead of beam velocities. The most significant findings are:

1) The calculation of the full Reynolds stress tensor is possible with ADCPs of 6 beams or more. Having a vertical beam is important to measure directly the vertical component of the velocity and get a robust measurement of the surface elevation above the ADCP. An integrated 7-beam configuration with 6 slant beams and one vertical beam is probably the best compromise. It is available off-the-shelf.
2) The detection of the peak of the echo intensity corresponding to the water surface has been improved, using a masking technique, especially when the water surface is glassy.
3) The interpolation methods of the peak of the echo intensity to estimate the surface elevations have been improved. The asymmetric linear interpolation provides an estimate of the significant wave height that is as accurate as the quadratic interpolation for the 50 cm bins but using the 100 cm bin data.

VII. FUTURE WORK

The methods for improved detection and interpolation of the peak of the echo intensity have been developed and validated with measurements at SEM-REV, offshore test site exposed to swell but with small currents. Some further developments and validation are also required for the directional spectrum analysis.

Using the other datasets available through the MOREDATAS and THYMOTE projects, the new methods will be applied to 5- and 8-beam ADCP measurements within strong tidal stream sites: Fall of Warness (Scotland), Fair Head (Northern Ireland) and Raz Blanchard (France). The improved waves results for these sites can then be used to improve the estimations of the turbulence spectrum using methods to separate Doppler noise, wave orbital velocities and turbulence fluctuations.

Future validation of the method may also include measurements using the off-the-shelf 7-beam ADCP SeaSEVEN by ROWE Tech Inc.

APPENDIX A: REVISION AND EXTENSION OF VERMEULEN ET AL. 2011

The findings by Vermeulen et al [6] have been reviewed and the following issues were identified:

1) The contour lines in "Figure 2" from [6] show that the maximum range of valid data depends on the angle of rotation of the slave ADCP around the z-axis (φ_3). Actually the maximum range only depends on the pitch and rolls angles of the slave ADCP and the contour lines should be identical across all subplots as shown in Fig. 14.
2) In "Figure 2" from [6], the red square showing the chosen beam configuration seems to be misplaced. Indeed the tilt angles are $\varphi_2 = 0°$ and $\varphi_1 = 20°$ corresponding to the red square in Fig. 14.
3) The valid range quoted in [6] (section 4, $ 11) is 80% and correspond to the incorrect calculation identified in point 1 above. With $\varphi_1 = 20°$, one of the beam is at 40° from vertical leading to a maximum range of 77%
4) Investigations of determinant values in "Figure 2" from [6] and minimum measurable stresses in Figure 3 from [6] suggest that a factor "2" was forgotten in the matrix $\boldsymbol{V}$ as in Equation (A1).

$$V(i) = T_{i,1}T_{i,1}\,\overline{u'^2} + T_{i,2}T_{i,2}\,\overline{v'^2} + T_{i,3}T_{i,3}\,\overline{w'^2} + 2\,T_{i,1}T_{i,2}\,\overline{u'v'} + 2\,T_{i,1}T_{i,3}\,\overline{u'w'} + 2\,T_{i,2}T_{i,3}\,\overline{v'w'} \quad (i = 1 \ldots 8) \tag{A1}$$

The "Figure 3" from [6] giving the minimum measurable stresses was extended to include all 6 stresses (Fig. 15).

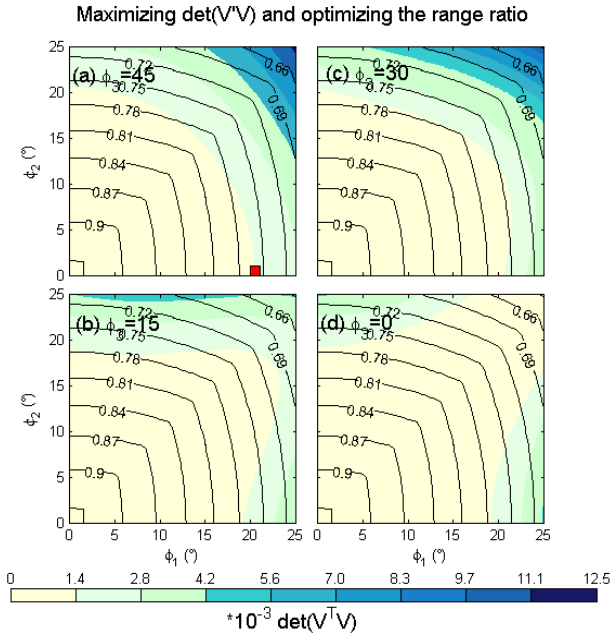

Fig. 14. Equivalent of Figure 2 from [6] but with correction of the maximum range (black contours), beam configuration chosen (red square) and determinant including the factor "2" in V matrix (coloured shades).

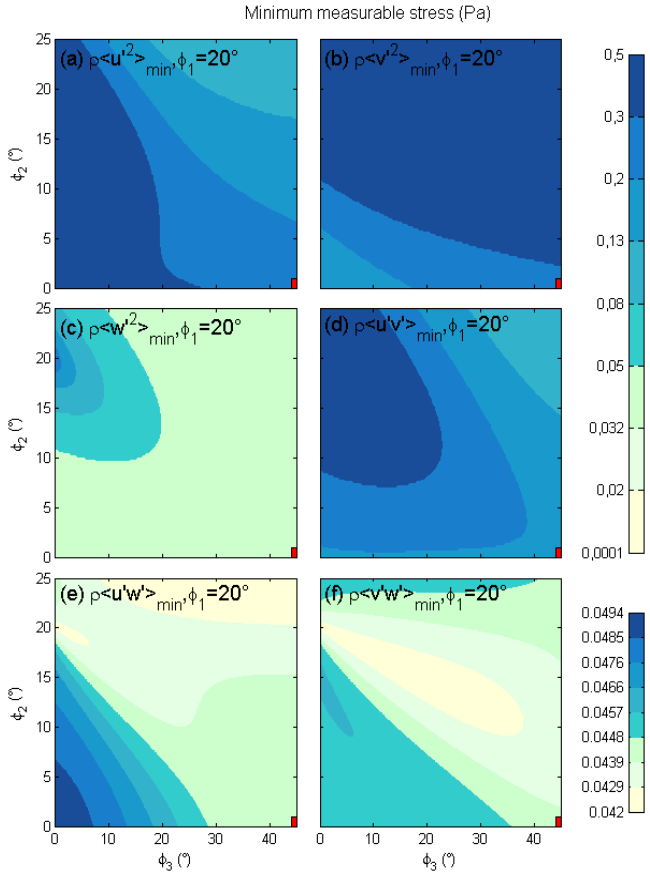

Fig. 15. Equivalent of Figure 3 from [6] but with V matrix including the factor "2" and extended to include values for the vertical shear stresses.

Unfortunately some unexplained discrepancies remained on the minimum measurable stresses between our calculation and [6]. This may be due to the use of a different Doppler noise value and/or a different number of pings.

APPENDIX B: ASYMMETRIC LINEAR INTERPOLATION

The location of the peak of the echo intensity can be determined for an asymmetric echo intensity using a least-squares fit for the three data points (y_1, y_2, y_3) around the peak, which is illustrated in Fig. 16.

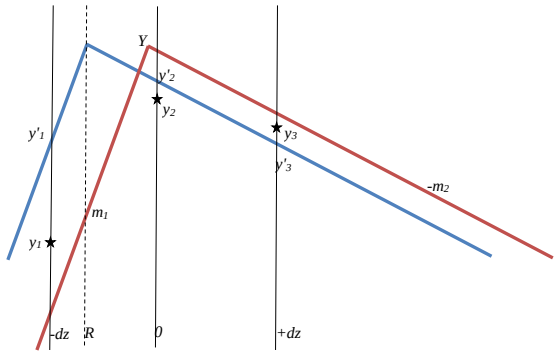

Fig. 16. Model of asymmetrical linear interpolation.

The values of the two asymmetrical slopes (m_1, m_2) can be estimated as the minimisation of (B1)

$$\epsilon = \sum_{i=1}^{3} (y_i' - y_i)^2 \tag{B1}$$

The coordinates for the position of y_i' can be obtained from geometry as one of two cases

$$y_1' = Y - m_1(\delta z + R) \tag{B2}$$

$$y_2' = Y + m_{1/2}R \tag{B3}$$

$$y_2' = Y - m_2(\delta z - R) \tag{B4}$$

Where when $-\delta z < R < 0$ (the blue line in Fig. 16) then $m_{1/2} = +m_2$ and when $0 < R < +\delta z$ (the red line in Fig. 16) then $m_{1/2} = -m_1$.

The sum of errors is then given by

$$\begin{aligned}\epsilon = {} & (Y - m_1(\delta z + R) - y_1)^2 \\ & + \left(Y - m_{1/2}R - y_2\right)^2 \\ & + (Y - m_2(\delta z - R) - y_3)^2\end{aligned} \tag{B5}$$

The minimum error can be identified by differentiating this with respect to Y and R and setting these to zero. First differentiating with respect to R

$$\begin{aligned}\frac{d\epsilon}{dR} = {} & -2m_1(Y - m_1(\delta z + R) - y_1) \\ & - 2m_{1/2}\left(Y - m_{1/2}R - y_2\right) \\ & + 2m_2(Y - m_2(\delta z - R) \\ & - y_3) = 0\end{aligned} \tag{B6}$$

Which can be factored and simplified to

$$A_R Y + B_R R + C_R = 0 \tag{B7}$$

Where

$$A_R = m_2 - m_{1/2} - m_1 \tag{B8}$$

$$B_R = m_1^2 + m_{1/2}^2 + m_2^2 \tag{B9}$$

$$C_R = (m_1^2 - m_2^2)\delta z + m_1 y_1 + m_{1/2} y_2 - m_2 y_3 \tag{B10}$$

Now differentiating with respect to Y

$$\begin{aligned} \frac{d\epsilon}{dY} = {} & 2(Y - m_1(\delta z + R) - y_1) \\ & + 2\big(Y - m_{1/2} R - y_2\big) \\ & + 2(Y - m_2(\delta z - R) - y_3) \\ & = 0 \end{aligned} \tag{B11}$$

Which can be factored and simplified to

$$A_Y Y + B_Y R + C_Y = 0 \tag{B12}$$

Where

$$A_Y = 3 \tag{B13}$$

$$B_Y = m_2 - m_{1/2} - m_1 \tag{B14}$$

$$C_Y = -(m_1 + m_2)\delta z - \sum_{i=1}^{3} y_i \tag{B15}$$

It can be shown that both of these functions are concave and must contain a single minimum. Solving for (B7) and (B12) then

$$R = \frac{C_Y A_R - C_R A_Y}{B_R A_Y - B_Y A_R} \tag{B16}$$

$$Y = -\frac{B_Y}{A_Y}\frac{C_Y A_R - C_R A_Y}{B_R A_Y - B_Y A_R} - \frac{C_Y}{A_Y} \tag{B17}$$

The gradients of the two slopes either side of the peak is then varied to minimize the error and so provide a best estimate for the location of the peak.

ACKNOWLEDGEMENT

We thank Gérard Le Bihan, Hugo Lugez, and Antoine Bertholon for assistance in the field. We acknowledge Teledyne RDI for their support in configuring ADCPs and using WavesMon. We also acknowledge ROWE Tech Inc to discuss feasibility of high frequency measurements with the SeaSEVEN ADCP.

REFERENCES

[1] Y. Lu and R. G. Lueck, "Using a Broadband ADP in a tidal channel. Part II: Turbulence," in *Journal of Atmospheric and Oceanic Technology*. Volume 15, November 1999

[2] M. T. Stacey, "Turbulent mixing and residual circulation in a partially stratified estuary", Ph.D. thesis, Stanford University, USA, 1996

[3] A. C. Whipple and R. A. Luettich Jr, "A comparison of acoustic turbulence profiling techniques in the presence of waves", in *Ocean Dynamics*, 50:719-729. DOI 10.1007/s10236-009-0208-3, 2009

[4] R. Dewey and S. Stringer, "Reynolds stresses and turbulent kinetic energy estimates from various ADP beam configurations: Theory", in *Journal of Physical Oceanography*, December 2007

[5] M. Togneri et al, " Comparison of 4- and 5-beam acoustic Doppler current profiler configurations for measurement of turbulent kinetic energy", in *Energy Procedia*, Volume 125, Pages 260-267, September 2017

[6] B. Vermeulen et al, "Coupled ADCPs can yield complete Reynolds stress tensor profiles in geophysical surface flows", in *Geophysical Research Letters*, Vol 38, L06406, DOI:10.1029/2011GL046684, 2011

[7] E. Droniou et al, "Waves and turbulence analysis of 8-beam ADCP measurements at EMEC's tidal test site: Fall of Warness", unpublished, April 2011

[8] A. Pieterse et al, "Coupled ADCP Measurements for Tidal Turbulence Characterization", in *EWTEC, Cork, Ireland*, September 2017.

[9] E. A. Terray et al, "Measuring waves and currents with an upward-looking ADCP", in *IEEE 6th Working Conference on Current Measurement, San Diego, Ca, USA*, 1999

[10] A. Bouferrouk et al, "Field measurements of surface waves using a 5-beam ADCP", in *Journal of Ocean Engineering, Volume 112, pp173-184, 2016.*

[11] Y. Perignon, I. Le Crom, "Challenging best knowledge to real conditions on the marine test site SEM-REV", in EWTEC conference, Nantes, France, 2015